Hindawi Publishing Corporation
International Journal of Antennas and Propagation
Volume 2013, Article ID 694819, 8 pages
http://dx.doi.org/10.1155/2013/694819

Application Article

Analysis and Design of a Novel Compact Multiband Printed Monopole Antenna

Junjun Wang and Xudong He

EMC Lab, School of Electronic and Information Engineering, Beihang University, Beijing 100191, China

Correspondence should be addressed to Junjun Wang; wangjunjun@buaa.edu.cn

Received 7 December 2012; Revised 2 May 2013; Accepted 29 May 2013

Academic Editor: Renato Cicchetti

A compact multiband printed monopole antenna is presented. The proposed antenna, composed of a modified broadband T-shaped monopole antenna integrating some band-notch structures in the metallic patch, is excited by means of a microstrip line. To calculate the bandwidth starting frequency (BSF) of the T-shaped broadband antenna, an improved formula is proposed and discussed. The multiband operation is achieved by etching three inverted U-shaped slots on the radiant patch. By changing the length of the notch slots, operation bands of the multiband antenna can be adjusted conveniently. The antenna is simulated in Ansoft HFSS and then fabricated and measured. The measurement results show that the proposed antenna operates at 2.25–2.7 GHz, 3.25–3.6 Hz, 4.95–6.2 GHz, and 7-8 GHz, covering the operation bands of Bluetooth, WiMAX, WLAN, and downlink of X-band satellite communication system and thus making it a proper candidate for the multiband devices.

1. Introduction

With the rapid development of the communication technology, there is a great demand for antennas suitable to operate with dual- or multibands characteristics in wireless communication devices, such as mobile phones and laptops. Printed antennas have been paid great attention in recent years because of their compact size, low profile, light weight, and low cost. A great quantities of printed antennas for dual- or multibands operations have been reported in the literature [1–12]. In [1–7], the authors have presented several kinds of printed monopole or dipole antennas for dual-band operation. In [8–12], slot antennas have been utilized. Antennas mentioned above achieve dual- or multibands operation; however, they usually have complicated structures or narrow bandwidth, and their operation bands cannot be adjusted easily either.

Recently, a lot of wideband antennas have been proposed because of the wide operation band and high date rate [13–15]. To avoid the interference between UWB (ultrawideband) antennas and narrow bandwidth communication systems, antenna designers have proposed several UWB antennas with band-notch characteristics [16–19]. The above-mentioned design solutions provide us a different way to achieve the multiband operation.

In this paper, we present a novel compact multiband monopole antenna based on the broadband antenna theory and employing band-notch technique. A T-shaped monopole antenna is designed to achieve a broad impedance bandwidth. Using the techniques suitable to widening of the operative frequency band, three inverted U-shaped slots are etched on the metallic patch to reject the undesired bands; in this way the multiband operation is achieved. The operation bands of the proposed antenna can be adjusted conveniently by changing the length of each band-notch slot.

The organization of the paper is as follows. In Section 2, the configuration of the proposed antenna is introduced. An improved formula for computing the bandwidth starting frequency (BSF) with higher accuracy is proposed and discussed. Then the broadband characteristic of the T-shaped monopole antenna is analyzed. Finally, the frequency behaviour of the band-notch structures consisting of three inverted U-shaped slots etched on the metallic patch is investigated. Results of the proposed antenna (return loss, normalized radiation pattern, and peak gain) are presented and discussed in Section 3, while some conclusions are drawn in Section 4.

Table 1: Optimized geometrical parameters of the proposed multiband antenna.

Parameters	W	w_1	w_2	w_f	L	l_1	l_2	l_g	l_{n1}	l_{n2}	l_{n3}	w_{n1}	w_{n2}	w_{n3}	d_1	d_2	d_3	g
Values (mm)	30	11.5	21.5	1.5	40	10	19	5	32	23	16	18	12	6	26.5	20.5	14.5	2

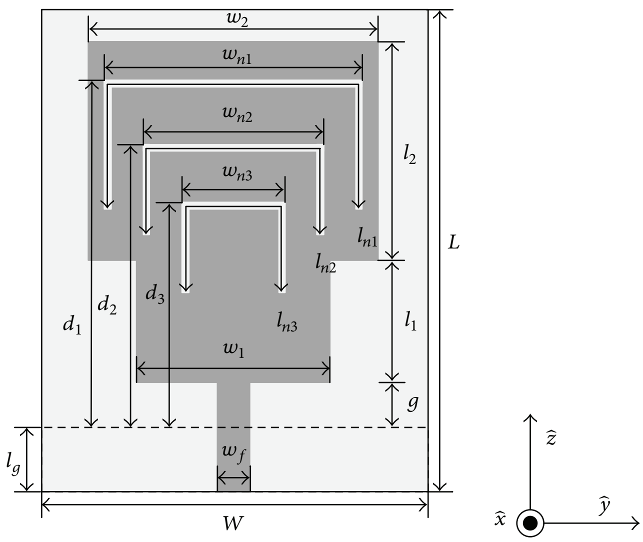

Figure 1: Geometry of the proposed multiband antenna.

2. Antenna Analysis and Design

Figure 1 shows the geometry of the proposed multiband antenna. The proposed antenna is printed on a low-cost FR4 substrate with relative permittivity of 4.4, dielectric loss tangent of 0.02, and thickness of 1 mm. A T-shaped patch is printed on one side of the substrate and a truncated ground plane on the other. The T-shaped patch is realized by removing two symmetric metal notches at the bottom of a rectangular patch in order to improve significantly the impedance matching of the monopole antenna at high frequency. Three inverted U-shaped slots with different sizes are etched on the T-shaped patch to reject the undesired frequency bands of the proposed multiband antenna. The commercial software Ansoft HFSS has been adopted for the analysis and design of the proposed antenna. The optimized geometrical parameters describing the antenna are reported in Table 1.

An improved formula useful to calculate the BSF in terms of the antenna parameters is proposed and discussed firstly. Then the effects of the antenna parameters are investigated. Finally, the inverted U-shaped band-notch structures are studied.

2.1. Improved Formula for BSF of the Broadband Antenna. For a broadband antenna, the BSF and bandwidth are two important factors to evaluate its frequency performance. An accurate formula to calculate BSF of a broadband antenna is quite necessary for antenna designers to save simulation time and accelerate the design process. In this paper, an improved formula is presented to provide a much more accurate prediction of BSF of the T-shaped monopole.

Kumar and Ray have proposed a formula to calculate the BSF of the planar monopole [19]. Thomas and Sreenivasan improved the formula by considering the effect of the substrate [20]. Equation (1) is the formula proposed by Thomas and Sreenivasan:

$$\text{BSF} = \frac{72}{l + r + g}\ \text{GHz}, \tag{1}$$

where l denotes the length of the monopole (both the planar monopole and the equivalent cylinder monopole), g denotes the gap between the ground plane and the monopole, and r denotes the radius of the equivalent cylinder monopole. The equivalent radius r is expressed as

$$r = \frac{A}{2\pi l \sqrt{\varepsilon_e}}, \tag{2}$$

where A denotes the area of the radiant patch and the area of the side face of the equivalent cylinder monopole, ε_e is the effective dielectric constant of the air-substrate composite dielectric and can be calculated by $\varepsilon_e = (1 + \varepsilon_r)/2$, and ε_r denotes the relative constant of substrate. The parameters l, r, and g appearing in (1) and (2) are expressed in millimeters.

However, (1) is not accurate enough to calculate the BSF of the T-shaped monopole antenna because the parameter g does not take into account the effect of the two bevel cuts on the feeding gap. Therefore, we propose to replace it by an effective parameter g_e defined as follows:

$$g_e = g + l - \frac{A}{w_2}. \tag{3}$$

Here w_2 denotes the width of the higher edge of the radiant patch, and g, l, and A have the same meanings as in (1), while in this paper, $l = l_1 + l_2$ and $A = w_1 l_1 + w_2 l_2$. Then (3) can be rewritten as

$$g_e = g + l_1 - \frac{w_1 l_1}{w_2}. \tag{4}$$

The modified formula to calculate BSF of the T-shaped monopole is

$$\text{BSF} = 72 \left(2l_1 + l_2 - (w_1 l_1 / w_2) + g + \left((w_1 l_1 + w_2 l_2) / \pi (l_1 + l_2) \sqrt{2\varepsilon_r + 2}\right)\right)^{-1} (\text{GHz}). \tag{5}$$

After performing some numerical simulations it is found that the values of the BSF calculated by (5) are smaller than

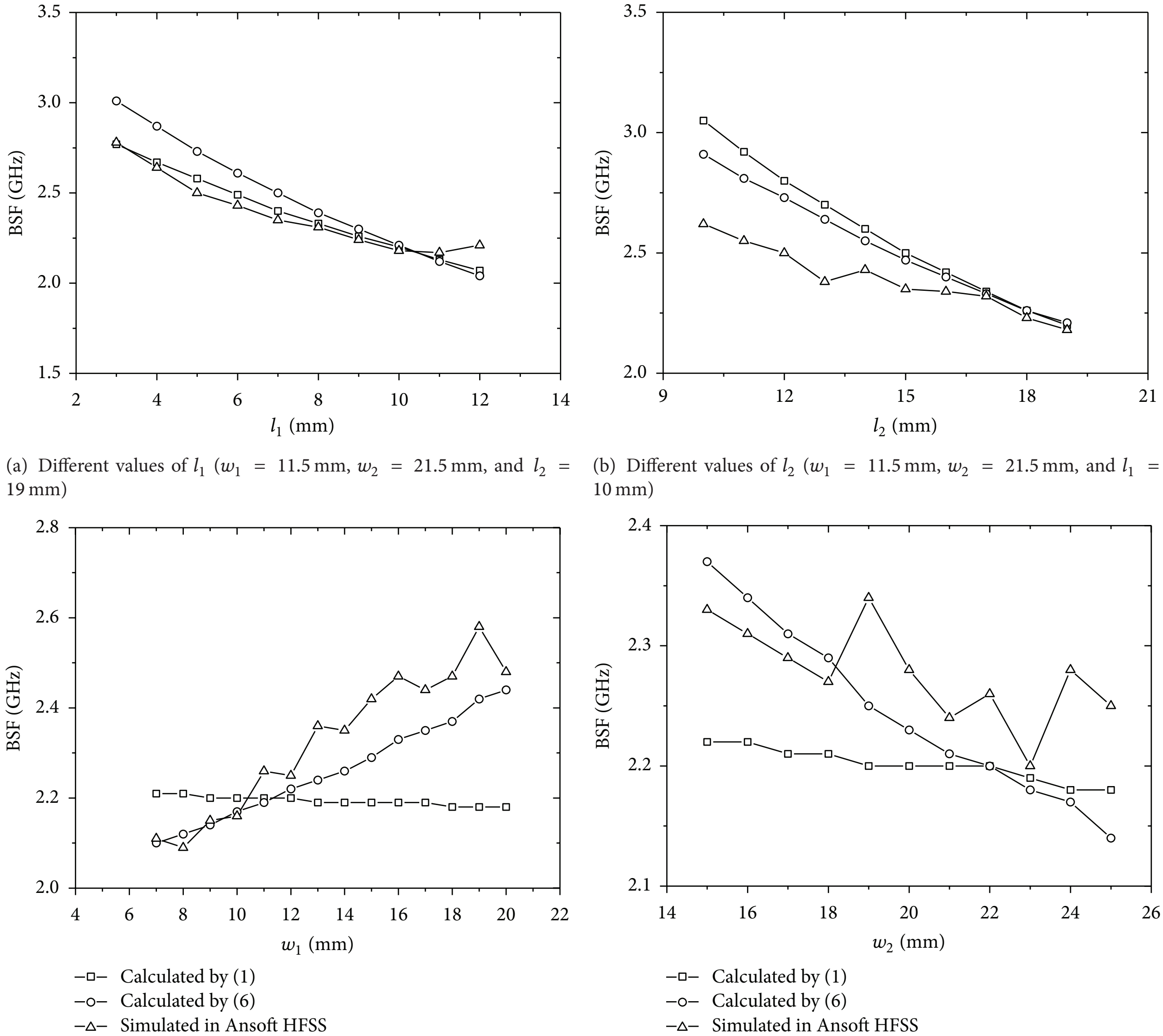

(a) Different values of l_1 (w_1 = 11.5 mm, w_2 = 21.5 mm, and l_2 = 19 mm)

(b) Different values of l_2 (w_1 = 11.5 mm, w_2 = 21.5 mm, and l_1 = 10 mm)

(c) Different values of w_1 (w_2 = 21.5 mm, l_1 = 10 mm, and l_2 = 19 mm)

(d) Different values of w_2 (w_1 = 11.5 mm, l_1 = 10 mm, and l_2 = 19 mm)

Figure 2: Calculated and simulated BSF for different values of the geometrical parameters.

the simulated ones. So a calibration factor F_c with its value of 1.145 is introduced. Then (5) can be modified as

$$\mathrm{BSF} = 72F_c\left(2l_1 + l_2 - (w_1 l_1/w_2) + g + \left((w_1 l_1 + w_2 l_2)/\pi(l_1+l_2)\sqrt{2\varepsilon_r+2}\right)\right)^{-1} \text{ (GHz)}. \quad (6)$$

Figure 2 shows the calculated and simulated BSF of the T-shaped monopole with different l_1, l_2, w_1, w_2, respectively, while the other parameters of the broadband antenna stay unchanged. From Figures 2(a) and 2(b) it can be observed that, for l_1, l_2, the values of BSF calculated by (1) and (6) almost have the same accuracy. For w_1, w_2, however, the values of BSF calculated by (6) are obviously much more accurate than those calculated by (1) compared to the simulated ones as shown in Figures 2(c) and 2(d), validating the accuracy of (6). The relative error of the proposed BSF formula comparing with the simulation is calculated; the maximum and mean values are 11.07% and 4.06%, respectively.

2.2. Broadband Antenna Design. In this section, the parameters of the broadband antenna are analyzed and discussed in detail. Figure 3 shows the frequency behavior of the scattering parameter S_{11} for the different dimensions of the T-shaped structure. From Figures 3(a) and 3(b), it can be observed that the two cuts at the lower edge of the radiant patch have a significant effect on the impedance matching at higher frequency. Correspondingly, the impedance match at higher frequency is improved. It is also seen in Figures 3(a) and 3(b)

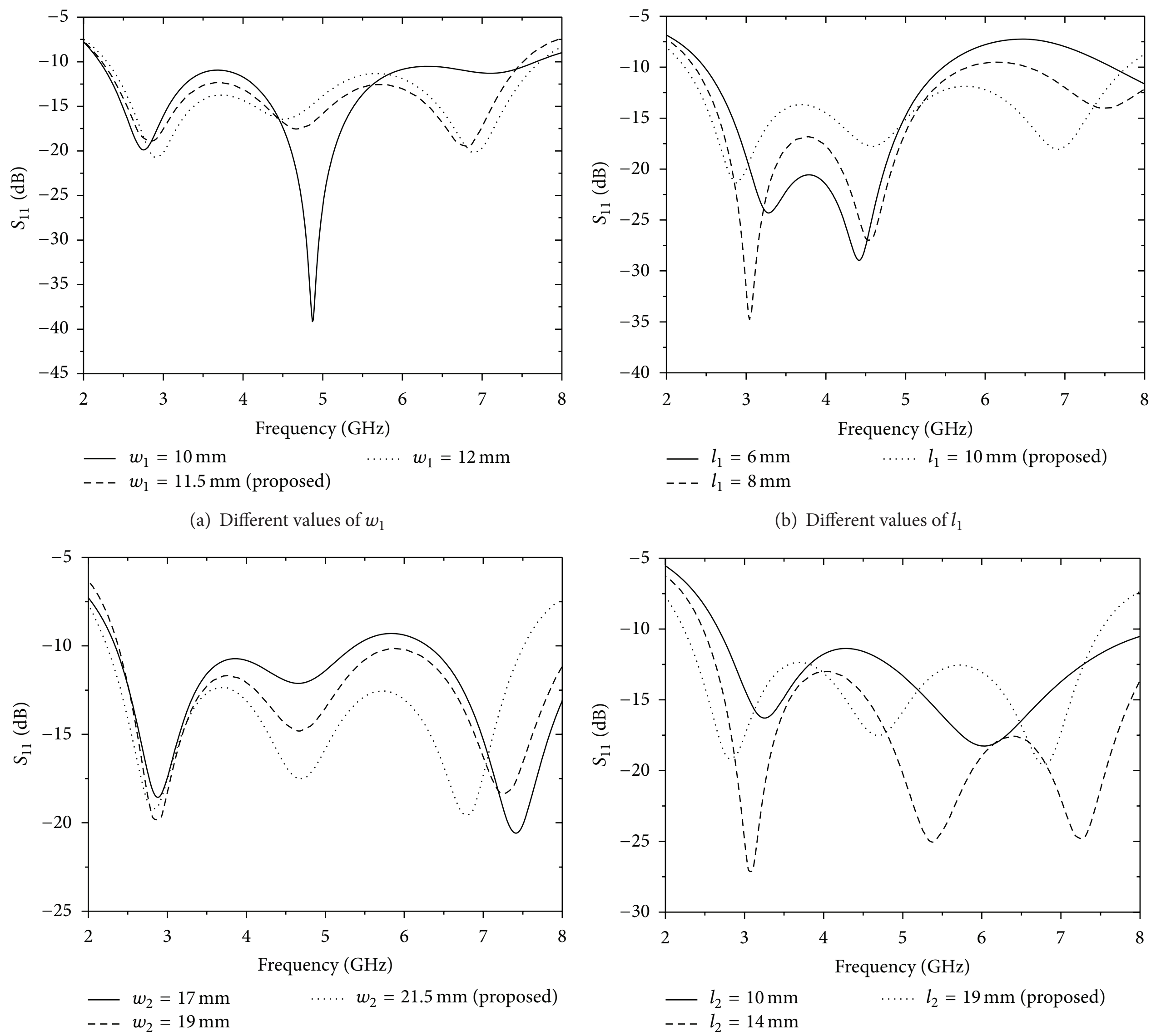

(a) Different values of w_1

(b) Different values of l_1

(c) Different values of w_2

(d) Different values of l_2

Figure 3: Frequency behavior of the scattering parameter S_{11} of the T-shaped antenna for different values of the geometrical parameters.

that the BSF of the broadband antenna decreases when w_1 decreases or l_1 increases. The reason is that the effective gap between the ground plane and the radiant patch increases while the width or length of the cuts increases. Because of the same reason, the BSF decreases when w_2 increases as shown in Figure 3(c) and when l_2 increases as shown in Figure 3(d), and we can see that with the increase of l_2, the BSF of the monopole antenna decreases and the impedance matching at higher frequency degrades. Because longer l_2 provides a longer current path at lower frequency, thus a lower BSF.

2.3. Multiband Antenna Design. Based on the broadband antenna design, three inverted U-shaped slots are etched on the T-shaped radiant patch to reject the undesired frequency bands, thus achieving the multiband operation. The resonant frequency of each inverted U-shaped slot can be approximately calculated by (7) reported in [21]:

$$f_{ni} = \frac{150}{l_{ni}\sqrt{\varepsilon_e}} \text{ GHz}, \tag{7}$$

where f_{ni} denotes the resonant frequency of the ith band-notch structure and l_{ni} denotes the length, expressed in millimeters, of the ith band-notch structure with $i = 1, 2, 3$. Equation (7) predicts a decrement of the resonant frequency f_{ni} as the parameter l_{ni} is increased.

Figure 4 shows the frequency behavior of the scattering parameter S_{11} for different values of the geometrical parameters l_{n1}, l_{n2}, and l_{n3}. It can be seen that with the increase of the length of the band-notch structures, the resonant frequency decreases and the bandwidth also changes, verifying the behavior predicted by (7). It is also found that the

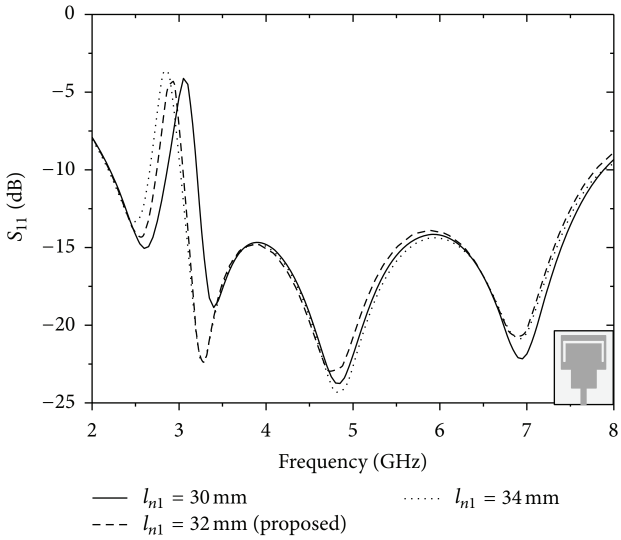

(a) With U-slot1

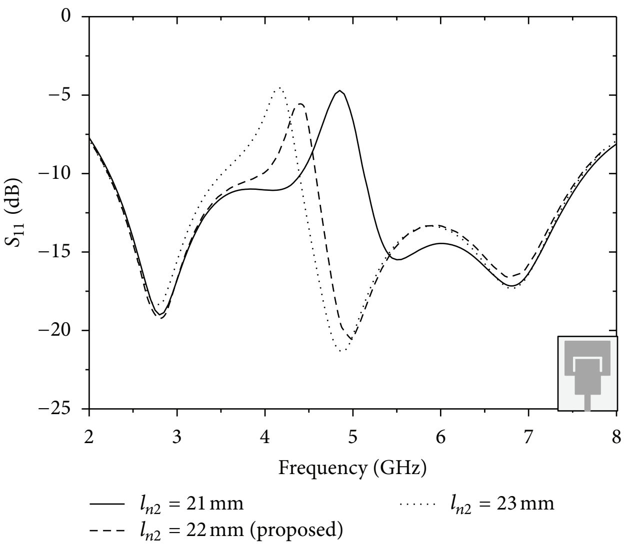

(b) With U-slot2

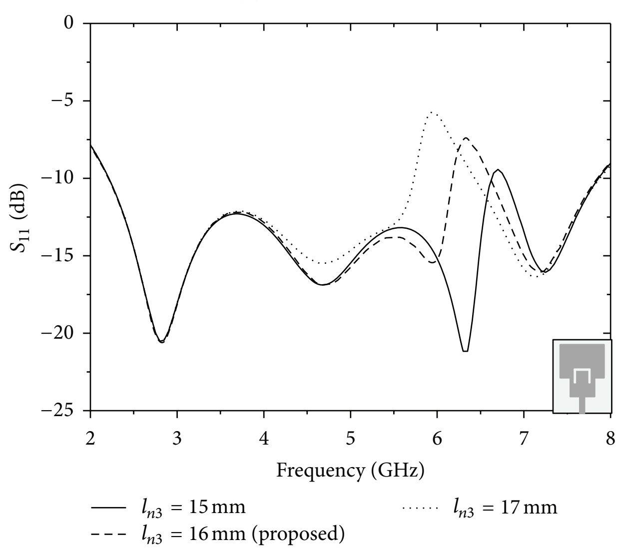

(c) With U-slot3

FIGURE 4: Frequency behavior of the scattering parameter S_{11} for different values of the geometrical parameters.

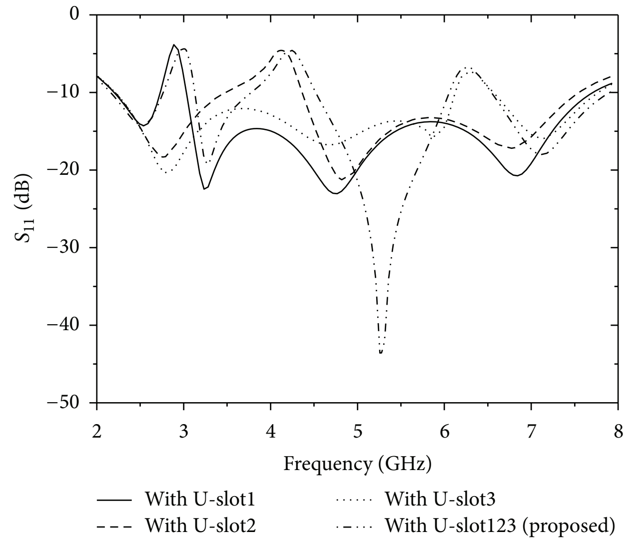

FIGURE 5: Frequency behavior of the scattering parameter S_{11} for the multiband antenna with one, two, and three U-slots.

width w_{ni} and the position d_{ni} of the inverted U-slots also have effects on the frequency performance of the band-notch structures, with $i = 1, 2, 3$.

Figure 5 shows the frequency behavior of the scattering parameter S_{11} of the broadband antenna with only one inverted U-shaped slot and with all the three slots (the proposed multiband antenna). It can be seen that each band-notch structure can work independently and has little effect on the frequency performance of the other band-notch structures.

The maps of the surface current distributions, excited on the monopole antenna at each one of the operative frequency bands, are shown in Figure 6.

3. Results and Discussion

The proposed antenna has been fabricated and then measured using Agilent Vector Network Analyzer E5071C. Figure 7 shows the simulated and measured S_{11} of the proposed multiband antenna. It can be seen that reasonable agreement has been achieved between the simulated and measured results. Because of the fabrication tolerances and of the perturbation effect caused by the SMA connector, there are some discrepancies between the two results. The fluctuation of relative permittivity and loss tangent of the FR4 substrate at high frequency also contributes to the disagreement.

The radiated electric field has a linear polarization for the proposed antenna. Figure 8 shows the computed radiation patterns of the proposed antenna at the working frequency of 2.4, 3.5, 5.5, and 7.5 GHz. It can be seen that the proposed antenna, similar to the typical monopole antennas, has nearly omnidirectional radiation pattern on H-plane except at 7.5 GHz. The degradation at 7.5 GHz can be explained as the following: with the increasing frequency the electrical length of the antenna is more than the half wavelength; then the surface current distributed on the radiant patch will be destructive, thus degradation of the radiation pattern at this frequency is observed.

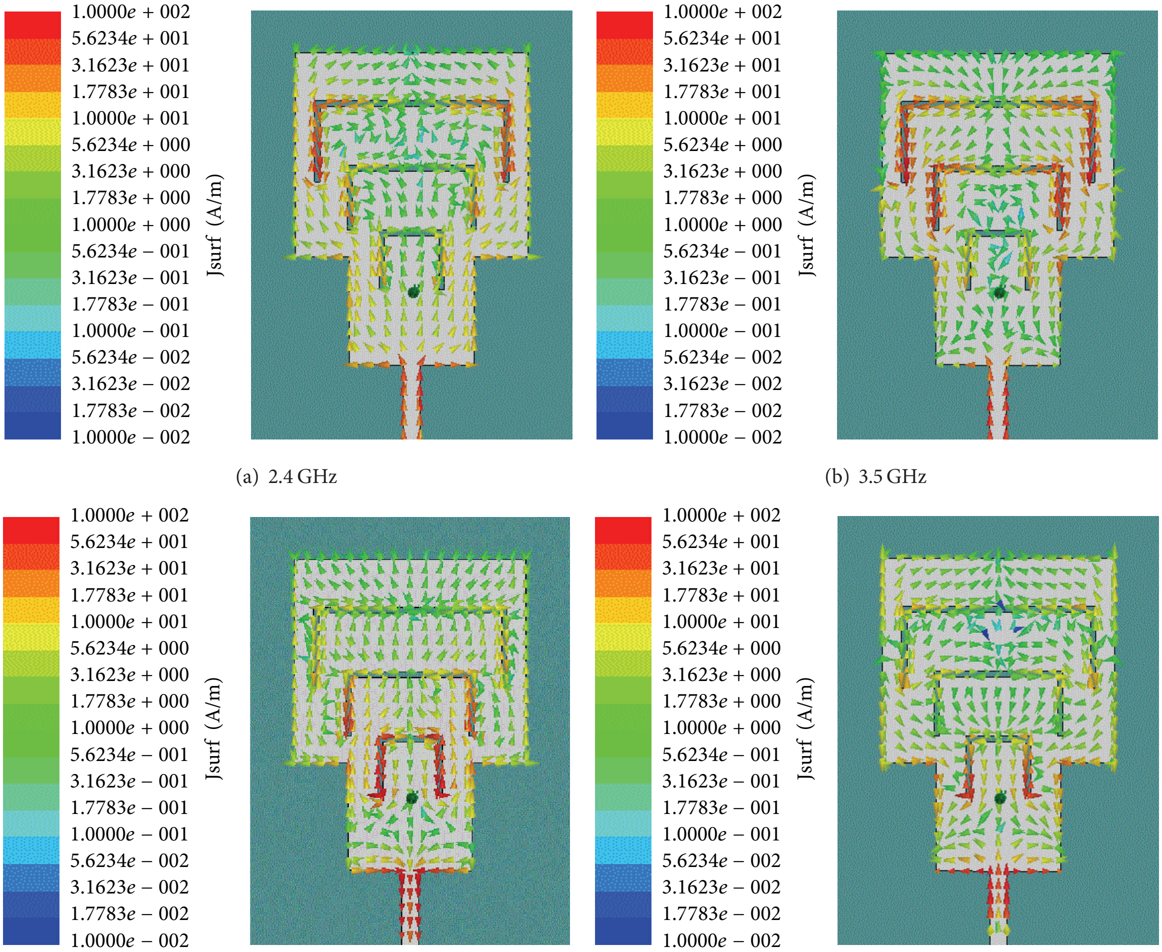

(a) 2.4 GHz (b) 3.5 GHz

(c) 5.5 GHz (d) 7.5 GHz

FIGURE 6: Maps of the surface current distributions at the frequency of (a) 2.4 GHz, (b) 3.5 GHz, (c) 5.5 GHz, and (d) 7.5 GHz.

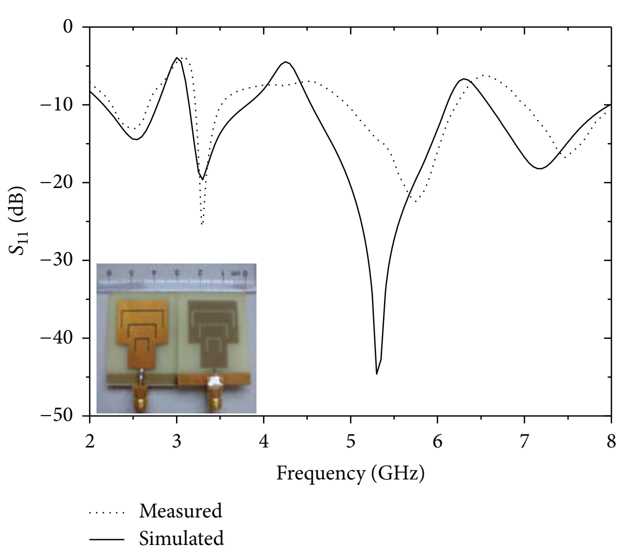

FIGURE 7: Frequency behavior of the simulated and measured S_{11} parameter of the proposed multiband antenna.

Figure 9 shows the simulated peak gain of the multiband antenna at the proposed frequency band. From the figure it appears that the peak gain increases as the frequency increases. The deviation between the maximum and minimum peak gain in each operation band is less than 1.5 dBi.

4. Conclusion

A multiband antenna based on a broadband antenna and the band-notch structures has been presented. A compact T-shaped monopole antenna with three inverted U-shaped slots has been adopted to achieve a multiband frequency behavior. After simulation and optimization in Ansoft HFSS, the proposed antenna is fabricated and measured. The measured results have shown that the frequency range of the proposed antenna can cover the operation bands of Bluetooth (2.4–2.484 GHz), WiMax (3.3–3.69 GHz), WLAN (5.15–5.875 GHz), and downlink of X-band satellite communication system (7.25–7.75 GHz). An improved formula useful to calculate the BSF of a general the T-shaped monopole

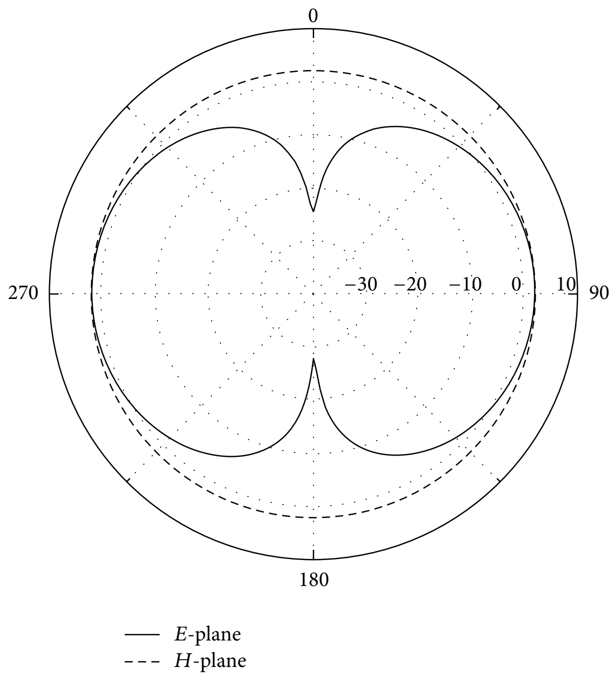

(a) 2.4 GHz

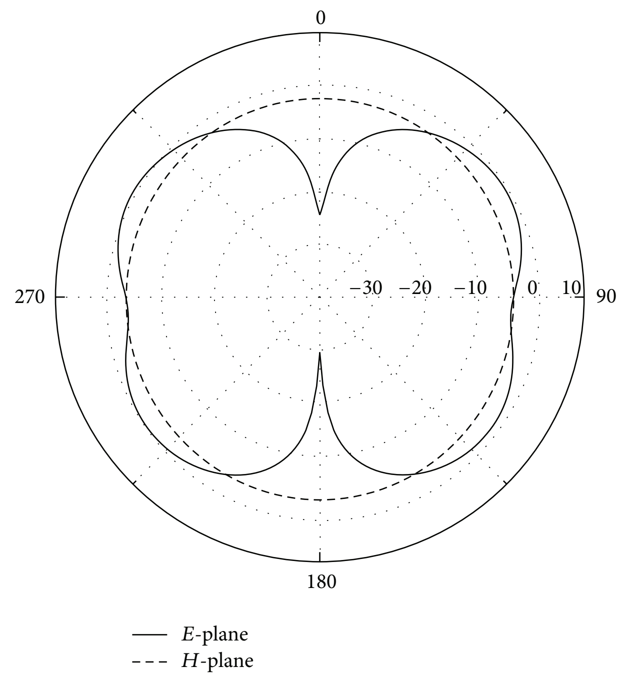

(b) 3.5 GHz

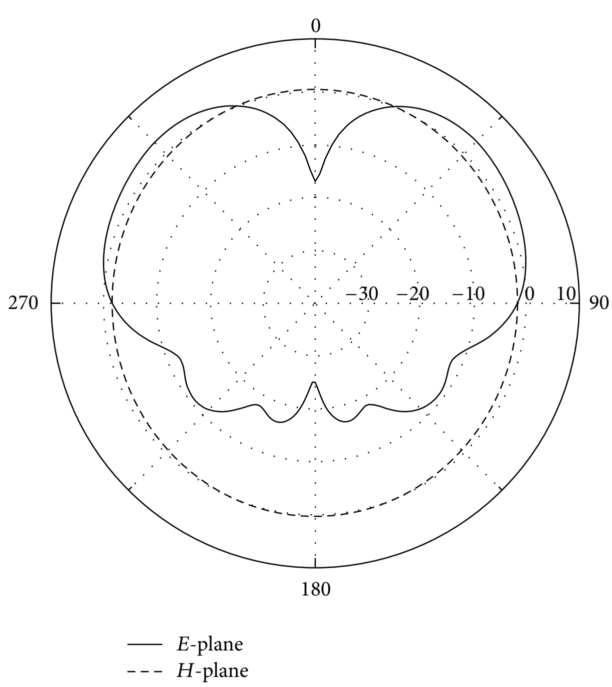

(c) 5.5 GHz

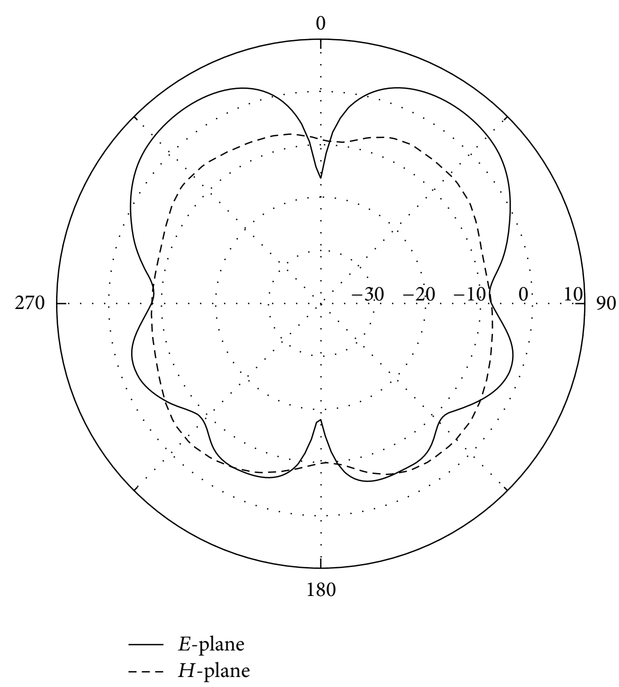

(d) 7.5 GHz

FIGURE 8: Simulated gain patterns in the *E*-plane (phi = 90 degree) and *H*-plane for the proposed antenna at the frequency of (a) 2.4 GHz, (b) 3.5 GHz, (c) 5.5 GHz, and (d) 7.5 GHz.

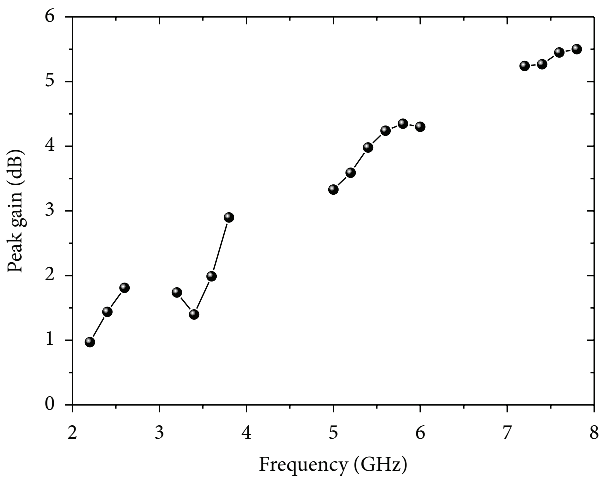

Figure 9: Peak gain for the proposed antenna.

antenna has been proposed and discussed. Comparison between the simulated and calculated BSF with different parameters of the T-shaped monopole has shown the good accuracy of the modified formula presented in this work.

Conflict of Interests

The authors declare that they have no conflict of interests with software Ansoft HFSS, in this paper.

References

[1] A. Mehdipour, A. R. Sebak, C. W. Trueman, and T. A. Denidni, "Compact multiband planar antenna for 2.4/3.5/5.2/5.8-GHz wireless applications," *IEEE Antennas and Wireless Propagation Letters*, vol. 11, pp. 144–147, 2012.

[2] F. Mirzamohammadi, J. Nourinia, and C. Ghobadi, "A novel dual-wideband monopole-like microstrip antenna with controllable frequency response," *IEEE Antennas and Wireless Propagation Letters*, vol. 11, pp. 289–292, 2012.

[3] M. J. Kim, C. S. Cho, and J. Kim, "A dual band printed dipole antenna with spiral structure for WLAN application," *IEEE Microwave and Wireless Components Letters*, vol. 15, no. 12, pp. 910–912, 2005.

[4] O. Tze-Meng, T. K. Geok, and A. W. Reza, "A dual-band omni-directional microstrip antenna," *Progress in Electromagnetics Research*, vol. 106, pp. 363–376, 2010.

[5] K. G. Thomas and M. Sreenivasan, "Compact CPW-fed dual-band antenna," *Electronics Letters*, vol. 46, no. 1, pp. 13–14, 2010.

[6] N. Zhang, P. Li, B. Liu, X. W. Shi, and Y. J. Wang, "Dual-band and low cross-polarisation printed dipole antenna with L-slot and tapered structure for WLAN applications," *Electronics Letters*, vol. 47, no. 6, pp. 360–361, 2011.

[7] Y. L. Kuo and K. L. Wong, "Printed Double-T Monopole Antenna for 2.4/5.2 Ghz dual-band WLAN operations," *IEEE Transactions on Antennas and Propagation*, vol. 51, no. 9, pp. 2187–2192, 2003.

[8] W. C. Liu, C. M. Wu, and N. C. Chu, "A compact CPW-Fed slotted patch antenna for dual-band operation," *IEEE Antennas and Wireless Propagation Letters*, vol. 9, pp. 110–113, 2010.

[9] M. N. Mahmoud and R. Baktur, "A dual band microstrip-fed slot antenna," *IEEE Transactions on Antennas and Propagation*, vol. 59, no. 5, pp. 1720–1724, 2011.

[10] A. A. Gheethan and D. E. Anagnostou, "Broadband and dual-band coplanar folded-slot antennas (CFSAs)," *IEEE Antennas and Propagation Magazine*, vol. 53, no. 1, pp. 80–89, 2011.

[11] C. Hsieh, T. Chiu, and C. Lai, "Compact dual-band slot antenna at the corner of the ground plane," *IEEE Transactions on Antennas and Propagation*, vol. 57, no. 10, pp. 3423–3426, 2009.

[12] Y.-C. Lee and J.-S. Sun, "Compact printed slot antennas for wireless dual- and multi-band operations," *Progress in Electromagnetics Research*, vol. 88, pp. 289–305, 2008.

[13] M. R. Ghaderi and F. Mohajeri, "A compact hexagonal wide-slot antenna with microstrip-fed monopole for UWB application," *IEEE Antennas and Wireless Propagation Letters*, vol. 10, pp. 682–685, 2011.

[14] N. Chahat, M. Zhadobov, R. Sauleau, and K. Ito, "A compact UWB antenna for on-body applications," *IEEE Transactions on Antennas and Propagation*, vol. 59, no. 4, pp. 1123–1131, 2011.

[15] G. Cappelletti, D. Caratelli, R. Cicchetti, and M. Simeoni, "A low-profile printed drop-shaped dipole antenna for wide-band wireless applications," *IEEE Transactions on Antennas and Propagation*, vol. 59, no. 10, pp. 3526–3535, 2011.

[16] C. C. Lin, P. Jin, and R. W. Ziolkowski, "Single, dual and tri-band-notched ultrawideband (UWB) antennas using capacitively loaded loop (CLL) resonators," *IEEE Transactions on Antennas and Propagation*, vol. 60, no. 1, pp. 102–109, 2012.

[17] W. T. Li, Y. Q. Hei, W. Feng, and X. W. Shi, "Planar antenna for 3G/Bluetooth/WiMAX and UWB applications with dual band-notched characteristics," *IEEE Antennas and Wireless Propagation Letters*, vol. 11, pp. 61–64, 2012.

[18] A. A. Gheethan and D. E. Anagnostou, "Dual band-reject UWB antenna with sharp rejection of narrow and closely-spaced bands," *IEEE Transactions on Antennas and Propagation*, vol. 60, no. 4, pp. 2071–2076, 2012.

[19] G. Kumar and K. P. Ray, *Broad Band Microstrip Antennas*, Artech House, Boston, Mass, USA, 2003.

[20] K. G. Thomas and M. Sreenivasan, "A simple ultrawideband planar rectangular printed antenna with band dispensation," *IEEE Transactions on Antennas and Propagation*, vol. 58, no. 1, pp. 27–34, 2010.

[21] Q. X. Chu and Y. Y. Yang, "3.5/5.5 GHz dual band-notch ultra-wideband antenna," *Electronics Letters*, vol. 44, no. 3, pp. 172–174, 2008.